Orthogonal Time Frequency Space Modulation (OTFS) for Positioning Using LEO Satellites

Guillem Foreman-Campins
TAU Wireless Research Center
Tampere University
Universitat Autònoma de Barcelona
guillem.foremancampins@tuni.fi

José A. López-Salcedo
Universitat Autònoma de Barcelona
Bellaterra, Spain
jose.salcedo@uab.cat

Elena Simona Lohan
TAU Wireless Research Center
Tampere University
Tampere, Finland
elena-simona.lohan@tuni.fi

***Abstract*—This paper analyses the achievable delay and Doppler estimation accuracies and the Multipath Error Envelopes (MEE) of Low Earth Orbit (LEO) Position-Navigation-Timing (PNT) systems, using the novel Orthogonal Time Frequency Space (OTFS) modulation. In this paper we investigate the advantages the OTFS modulation, which has originally been designed for communication purposes, may bring to the positioning field in LEO-PNT systems, in particular in the presence of doubly-selective wireless fading channels exhibiting both delay and Doppler spreads. We show how a LEO air-to-ground channel fits this description due to its fast dynamics, and we present the improvements of using OTFS with respect to the standard spread-spectrum single-carrier Binary Phase Shift Keying (BPSK) modulation in terms of delay-Doppler estimation accuracy, in addition to a comparison of their performance in LEO multipath scenarios through their respective MEEs.**

I. Introduction

Wireless positioning by means of Global Navigation Satellite Systems (GNSS) has been the de-facto standard for outdoor positioning for many years [1], [2]. Nonetheless, the demands in the ever-increasing positioning field have put forward the need for systems with higher accuracy, while keeping a reduced complexity and thus, a smaller power-consumption footprint. A prominent solution comes from the use of alternative systems to complement the GNSS constellations. In particular, the use of Low-Earth-Orbit (LEO) satellites, now in the spot of the so-called NewSpace economy [3]–[5], can significantly contribute to improve the positioning solution.

The three most important challenges that satellite-based positioning must face in the coming years are: i) achieving good accuracy in indoor scenarios, ii) overcoming unintentional and intentional interferences, and iii) providing positioning solutions for devices with limited computational resources (e.g. as in the context of Internet of Things). LEO satellites are expected to solve the first two challenges due to their closer orbital distance to the Earth, and thus their closer proximity to user terminals, resulting in a greater received power; as for the third challenge, it is expected to be addressed by the use of new signaling formats specifically tailored to such new user requirements. Using LEO as an alternative positioning system is also expected to guarantee highly secure, sovereign, and global connectivity services to provide support to crisis management and protection of critical infrastructure. Due to the above-mentioned advantages, the use of LEO satellites for positioning is currently heavily investigated [3], [4], [6]–[8], still with many key aspects to be researched and covered. Particularly, there's no general consensus on the LEO-PNT signal design, which is still looking for an optimal trade-off [9]. To this end, this paper showcases the potential of the up-and-coming modulation first presented in [10], named Orthogonal Time Frequency Space (OTFS), and its adoption by future dedicated LEO Position-Navigation-Timing (LEO-PNT) satellites.

The main novel contributions of this paper are: i) investigating the potential of OTFS in the context of LEO-PNT systems (while OTFS has been studied so far with LEO signals for communication purposes [11], to the best of the Authors' knowledge, its potential as a positioning waveform in LEO-PNT systems has not yet been addressed in the open literature); ii) presenting the signal design and configuration of the OTFS modulation for positioning with high delay-Doppler estimation accuracy; iii) comparing the delay and Doppler accuracies and the Multipath Error Envelopes achievable with OTFS with a benchmark based on the spread-spectrum single-carrier BPSK modulation, used in all existing GNSS systems; the Cramer-Rao lower Bound (CRB) is also given for reference.

II. LEO-PNT concept and related work

LEO-PNT (Low Earth Orbit Positioning, Navigation, and Timing) refers to the use of satellites in low Earth orbit (LEO) to provide positioning, navigation, and timing services. Unlike traditional GNSS satellites, which operate in medium Earth orbit (MEO), LEO satellites orbit much closer to the Earth, typically at altitudes between 500 and 2000 kilometers above the Earth. Strictly speaking, LEO orbits start around 150 km above the Earth, but due to the strong Earth drag effect below 500 km, the commercially launched LEO satellites so far have been in orbits above 550 km [4], [9], [12]. Due to their proximity to Earth, LEO satellites can provide stronger signals and lower latencies compared to GNSS signals when similar carrier frequencies are employed [9]. LEO-PNT systems could also complement existing GNSS systems, providing additional signals that enhance overall accuracy and resilience against jamming and spoofing, which are highly desirable nowadays.

Most of the research dedicated to LEO-PNT so far has focused on using existing LEO constellations, such as the SpaceX Starlink, the Amazon Kuiper, or UK's Oneweb, as signals of opportunity and harnessing their potential for positioning through various Doppler-based positioning [7], [8] or cognitive processing approaches [6], [13]. LEO-PNT design as standalone systems has been addressed very little so far and the research has focused mainly on LEO-PNT constellation optimization [14] or on the systematic assessment of various LEO-PNT concepts, including orbit and constellation design, carrier frequency, bandwidth, and signal power issues [9].

Previous work focusing on LEO-PNT waveform modulation design is rather limited and can be found for example in [15] ,which focuses on Chirp Spread Spectrum (CSS) modulations, and in [16], focusing on direct-sequence spread spectrum BPSK modulation, which is also the waveform of choice in GNSS systems. For comparative purposes and also because CSS is a non-stationary modulation, we chose the direct-sequence spread spectrum BPSK as a benchmark in our studies. Related works have also focused on developing and optimizing the navigation payloads in LEO-PNT, without a particular attention to the modulation waveform; such works include the research on hosted payloads, designed to augment existing GNSS constellations with additional navigation signals from LEO satellites and which rely on GNSS for orbit determination and time synchronization, ensuring compatibility and interoperability [17]. There are currently no studies on standalone LEO-PNT navigation payloads to the best of the Authors' knowledge, though research efforts focused on such navigation payload design are undertaken in the INCUBATE project[1], which also sponsored this work.

III. OTFS MODULATION OVERVIEW

OTFS, initially designed as an evolution of Orthogonal Frequency Division Multiplexing (OFDM) for wireless communications, fundamentally aims at solving one of the key problems of the latter [18], the Inter-Carrier Interference (ICI) suffered under strong user dynamics [19]. OFDM systems may require complex equalization techniques and increased guard intervals to mitigate ICI effects [18], [20], which can reduce spectral efficiency and increase computational complexity [21].

In contrast, OTFS represents a relatively novel approach [20], [22], [23] introduced to address the intricate challenges that future wireless systems are expected to encounter, such as Doppler and delay spreads, and associated ICI and ISI effects. Unlike conventional methods such as single-carrier and OFDM communications, OTFS exploits better and jointly the time and frequency diversity, which aids in the management of ICI, offering promising capabilities in handling the demands of 6G networks, where it is standing as a solid candidate. The delay-Doppler representation in OTFS allows for more accurate channel estimation with lower training overhead, which is beneficial in dynamic environments.

[1]https://www.incubateproject.org/

Essentially, OTFS adds an extra layer to OFDM by translating a time-frequency signal into the so-called delay-Doppler (DD) domain, by means of the Inverse Symplectic Fourier Transform (ISFFT), or otherwise by directly converting from the time domain to the DD domain through the Zak transform. While OFDM divides the signal into various frequency subcarriers, OTFS adds the time layer into the modulation scheme by concatenating various OFDM symbols into one OTFS symbol, making the OTFS symbol longer and time-diverse. These translations manage to convert a time-variant channel into a non-variant sparse and separable set of taps in the delay-Doppler (DD) domain. Because of the way in which OTFS handles the longer symbol time with respect to OFDM, all the symbols in the DD domain experience the channel similarly, solving the limitation of OFDM of losing orthogonality when the channel dynamics are strong [24].

Notably, OTFS has received attention from multiple disciplines and not just 5G/6G communications, such as in the field of radar [22] or Internet of Things (IoT) [23]. However, its benefits as a positioning waveform have not been studied yet, to the best of the Authors' knowledge. This paper aims at extending OTFS for LEO-PNT-based positioning and investigating its potential as a waveform in future standalone LEO-PNT designs.

IV. OTFS SIGNAL MODEL

OTFS makes use of the delay-Doppler (DD) domain to obtain specific signal properties that make it robust towards channel impediments, particularly Doppler spreads and ICI. The discrete-time domain representation of the OTFS-modulated signal represented in Fig. 1 is given by $s(k)$,

$$X_{\text{TF}}[n,m] = \sum_{p=0}^{N-1}\sum_{q=0}^{M-1} X_{\text{DD}}[q,p]e^{j2\pi(\frac{mp}{N}-\frac{nq}{M})} \tag{1}$$

$$s(k) = \frac{1}{\sqrt{MN}}\sum_{k=0}^{N-1}\sum_{m=0}^{M-1} X_{\text{TF}}[k,m]e^{j2\pi\frac{m}{M}k} \tag{2}$$

with $X_{\text{DD}}[q,p]$ containing the $(M \times N)$ information-bearing symbols in the DD domain that are converted into a set of $(M \times N)$ time-frequency (TF) symbols $X_{\text{TF}}[k,m]$ in (1). The latter are then transmitted using the available bandwidth B, which is divided into a set of M equi-spaced subcarriers with separation $\Delta f = B/M$, over N consecutive time slots of duration T seconds each, known as the OTFS frame duration.

The TF symbols can be conveniently put in matrix form as,

$$\mathbf{X}_{\text{FT}} = \mathbf{F}_M \mathbf{X}_{\text{DD}} \mathbf{F}_N^H. \tag{3}$$

and the OTFS signal samples in (2) can be stacked into the $(MN \times 1)$ vector $\mathbf{s}$ as follows,

$$\mathbf{s} = \left[\mathbf{F}_M^H \mathbf{X}_{\text{FT}}(:,1) \ldots \mathbf{F}_M^H \mathbf{X}_{\text{FT}}(:,N)\right]^T \tag{4}$$

with $\mathbf{F}_Q$ the $(Q \times Q)$ discrete-time Fourier matrix, and simplified into the following compact expression,

$$\mathbf{s} = \text{vec}(\mathbf{F}_M^H \mathbf{X}_{\text{FT}}) = \text{vec}(\mathbf{X}_{\text{DD}} \mathbf{F}_N^H). \tag{5}$$

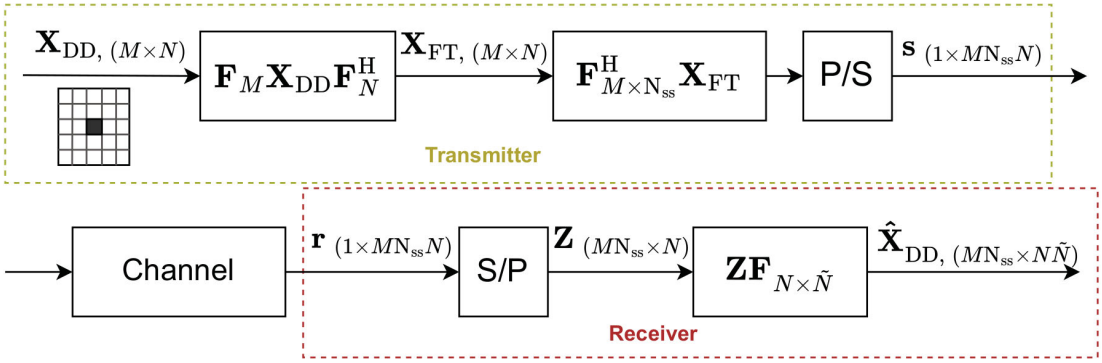

Fig. 1. OTFS block diagram with oversampling to get access to the underlying characteristics of the signal.

As can be seen, an OTFS frame can be regarded as a set of N consecutive pre-coded OFDM symbols. In the delay domain, the OTFS resolution is given by $\Delta\tau = 1/B$ while in the Doppler domain, this concatenation of OFDM symbols provides a Doppler resolution of $\Delta\nu = \frac{B}{MN}$. These resolutions define the DD grid where the symbols are placed, along with the M subcarriers and N concatenated OFDM symbols, which in turn give M delay grid points and N Doppler grid points.

In the sequel, we will consider the reception of the OTFS signal $s(k)$ over a multipath channel, leading to,

$$r(k) = \alpha s(k-\tau)e^{j2\pi k\nu} + \sum_{l=1}^{N_p} \alpha_l s(k-\tau-\tau_l')e^{j2\pi k(\nu+\nu_l')} + w(k) \tag{6}$$

which includes the Line-of-Sight (LOS) component, impacted by a delay τ and a Doppler shift ν, and with amplitude α, along with the N_p multipath components. The l-th multipath integrant has an amplitude α_l, and is affected by a relative delay τ_l' and a relative Doppler shift ν_l', which are relative to the LOS's τ and ν, respectively. Finally, $w(k)$ represents the receiver thermal noise.

V. OTFS Considerations for LEO-PNT

The benefits of using OTFS signals in a LEO context have already been shown for the case of Non-Terrestrial-Networks [25], where a gain is observed with respect to its OFDM counterpart due to the ICI induced by the high Doppler dynamics of the LEO satellite. The advantages for LEO positioning applications with OTFS have not been addressed yet, even though a relevant gain should be expected as well due to the time-varying relative Doppler between the LOS and the reflected paths caused by the fast-changing geometry.

For the sake of clarity in the subsequent analysis, we will consider an OTFS signal composed of a single pilot symbol in the DD domain without other data surrounding it, shown in Fig. 2. This figure exhibits the underlying characteristics of a pilot in the DD domain, which can be extrapolated to any data placed in this domain, which is comprised of a two-dimensional sinc in the delay-Doppler directions, whose zeroes appear at the integer points of the grid.

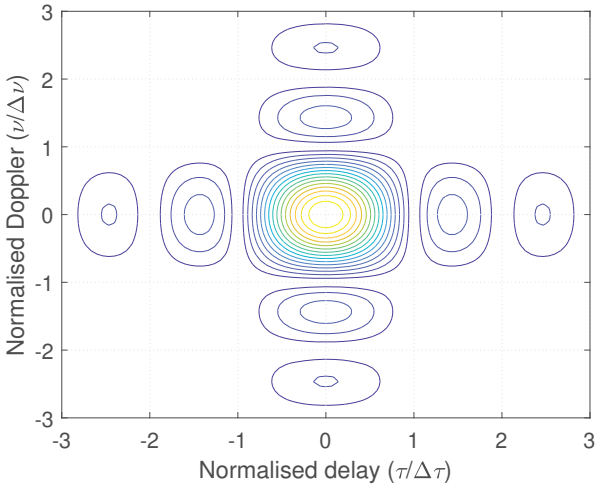

Fig. 2. Underlying characteristics of one OTFS pilot

To properly recover this pilot and be able to obtain accurate delay and Doppler estimates, we are implementing an oversampled receiver in the DD domain, which can be implemented through oversampled Fourier transforms in (3) and (4), as shown in Fig. 1. In particular, at the receiver, $\mathbf{F}_N$ can be applied with a larger number of points in order to oversample the Doppler domain, by computing $\hat{\mathbf{X}}_{\text{DD},M\times\tilde{N}} = \mathbf{ZF}_{N\times\tilde{N}}$, with $\tilde{N}$ the zero-padding factor and $\mathbf{Z}$ the received time-domain signal reshaped to an $M \times N$ matrix. For the delay domain, the oversampling can be applied similarly at transmission through $\mathbf{s} = \text{vec}(\mathbf{F}^{\text{H}}_{M\times N_{\text{ss}}}\mathbf{X}_{\text{FT}})$, with N_{ss} the number of samples per each embedded OFDM symbol in the OTFS frame.

The OTFS multipath mitigation properties have been studied in the literature for communications applications [26], [27], where a strong dependence on the OTFS signal design in the DD domain has been found. A similar study is presented next, but keeping in mind LEO-based positioning applications.

A. Representative scenario definition

In order to address the study of OTFS for LEO-based positioning applications, the one-ray multipath scenario considered

in [5] will be adopted. This scenario comprises one replica coming from the reflection of the transmitted signal onto an object separated a distance d from the receiver, and a receiver altitude of h_{RX}. Two different cases are considered herein, mainly depending on the satellite elevation θ_{el} at the moment of receiving the signal, and the distance d, as described in Table I.

TABLE I. SCENARIO DEFINITION FOR LEO-BASED POSITIONING

Scenario	d	h_{RX}	sat. height	sat. vel.	θ_{el}	Δd	f_c	ν'
1)	20 m	2 m	500 km	0.75 °/s	45º	$2d\cos(\theta_{\mathrm{el}})$	10 GHz	**14.6 Hz**
2)	30 m	2 m	500 km	0.75 °/s	60º	$2d\cos(\theta_{\mathrm{el}})$	12 GHz	**29 Hz**

Due to the fast-changing geometry caused by the rapid movement of the LEO satellite, the reflected ray will have quick changes in its amplitude and path length. These quick changes derive in a relative Doppler shift of the multipath with respect to the LOS, defined as $\nu' = \frac{f_c}{c} \cdot \frac{\partial \Delta d}{\partial t}$. Hence, a quick variation on the extra path length that the multipath travels with respect to that of the LOS will result in added relative Doppler shift in the multipath signal. The extra path length Δd of the multipath with respect to the LOS varies with θ_{el}, which in turn varies with time, depending on the satellite angular velocity, defined in $\mathrm{deg/s}$. Furthermore, the satellite angular velocity will be higher the lower the satellite altitude, and thus the relative Doppler shift ν' will be higher for lower-flying satellites.

We take two different scenarios with reflection distances, satellite elevations, and carrier frequencies, which are representative of real-case multipath scenarios.

They result in ν' values of 14.6 Hz and 29 Hz, respectively, which gives enough separation for the LEO multipath channel to be considered to be *doubly-spread*, that is, to be have paths that are distinguishable in both delay and Doppler directions. This gives an opportunity for OTFS to shine, given its characteristic time-frequency diversity, which endows it with a high Doppler resolution that can be able to discern the multipath in both delay and Doppler directions at the same time.

B. OTFS signal configuration

Let us consider a $B = 10$ MHz, a sampling frequency $F_s =$ 50 MHz, and the reception of one OTFS symbol. To make use of OTFS for the aforementioned LEO *doubly-spread* channel, the Doppler resolution defined as $\Delta\nu = \frac{B}{M \cdot N}$ should be small enough to tell apart the various paths in the Doppler domain.

Taking into account the obtained ν' values from Table I, a target value of $\Delta\nu = 15\,\mathrm{Hz}$ is chosen, which is small enough to avoid strong overlapping between the LOS and the multipaths in either of the two scenarios, so that the LOS can be distinguished clearly and little error is induced by the presence of multipath. While such a configuration will avoid overlapping of the main lobes of the LOS and the multipath signal due to $\Delta\nu$ being bigger than ν', it is notable that the multipath will have an impact nonetheless on the LOS, given the secondary lobes present in each component, as shown in Fig. 2. The impact of the multipath on the LOS will only be nought when ν' is an integer multiplier of $\Delta\nu$. This mitigation approach is not possible for other modulations that do not achieve time and frequency diversity, since the paths will not be distinguishable in the two dimensions.

For the considered B, and for a frequency subcarrier spacing of Δf = 15 kHz, following the OFDM standard in [28], a total of $M = 667$ subcarriers are deployed, which entails a frame duration of $T = 1/\Delta f = 66.7$ μs. This means that a total of $N = 1000$ need to be transmitted per OTFS frame in order to achieve the desired Doppler resolution $\Delta\nu$, with one OTFS symbol lasting $1/\Delta\nu$ = 66.7 ms, which is small enough for ν' to remain roughly constant and thus time-invariant for OTFS. Table II presents a summary on the configuration of the relevant OTFS parameters, namely N and M, for the given B, and the target $\Delta\nu$ considering the worst-case scenario from Table I.

TABLE II. OTFS PARAMETERS FOR THE WORST SCENARIO IN TABLE I

B	Δf	M	target $\Delta\nu$	needed N
10 MHz	15 kHz	$\frac{B}{\Delta f} = 667$	15 Hz	$\frac{B}{M\Delta\nu} = 1000$

VI. SIMULATION RESULTS

In this section, simulation results are presented for the OTFS performance in the LEO-based positioning scenarios defined in Section V-A with multipath. First off, though, we take a look at the performance of OTFS in a scenario without multipath. The results for OTFS will be compared with those obtained for the spread-spectrum single-carrier BPSK modulation widely used in GNSS. The Cramér-Rao Bound (CRB) will be considered as well as a reference benchmark.

A. Performance for the LOS-only channel

Let us first consider the case for an Additive White Gaussian Noise (AWGN) channel, i.e. without multipath, for the retrieval of the achievable accuracy of OTFS, and its comparison with BPSK and their respective CRBs. For OTFS, the delay and Doppler are estimated at the receiver in the DD domain, where only one DD symbol and a known position in the DD grid are transmitted. For BPSK, the delay and Doppler are estimated by computing the ambiguity function (AF) obtained by performing the correlation between the baseband received signal and the local replica (i.e. matched filter), for various tentative Doppler values.

For an AWGN channel, the CRB for time-delay estimation (i.e. ranging accuracy) is given by (7), with $\sqrt{\alpha}B/2$ the root-mean-square (RMS) bandwidth and E_s the received signal energy.

$$\mathrm{CRB}(\tau) = \left(\alpha (B/2)^2 \cdot \frac{E_s}{N_0/2} \right)^{-1} \tag{7}$$

Regarding the factor α, it can be approximated for OTFS and BPSK as $\alpha_{\mathrm{OTFS}} \approx \frac{4\pi^2}{3}$ and $\alpha_{\mathrm{BPSK}} \approx 4.41$, respectively [29], the difference coming from the better spectrum utilisation

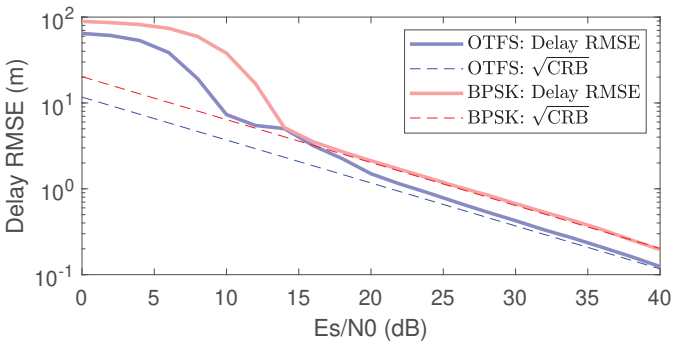

Fig. 3. Delay estimation accuracy comparison between OTFS, BPSK and their respective CRBs.

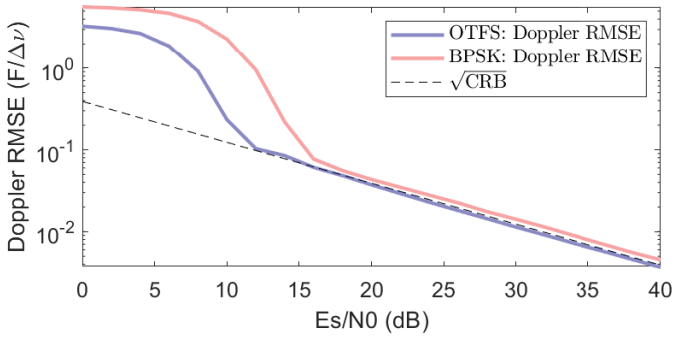

Fig. 4. Doppler estimation accuracy comparison between OTFS, BPSK and the CRB.

of OTFS with respect to BPSK. The α_{OTFS} is actually the same as that of OFDM, since OTFS can be understood as OFDM plus precoding. In order to make a fair comparison between OTFS and the spread-spectrum single-carrier BPSK, the latter is using a symbol rate $1/T = B/2$ and its spectrum is filtered so as to make sure that BPSK has the same two-sided bandwidth B used by OTFS.

With these considerations in mind, the results in Fig. 3 are obtained, showcasing the achievable delay RMS Error (RMSE). These results show that OTFS does not provide much advantage in ranging estimation with respect to BPSK in an AWGN channel, except for the better spectral usage that gives a larger RMS bandwidth, and thus better delay accuracy. These results should be expected, given that the CRB defined in (7) has little dependance on the modulation scheme, except for that given by α, and the pilot in the DD domain does not provide an advantage with respect to the AF of spread-spectrum BPSK in a multipath-less scenario.

Regarding the CRB for Doppler estimation, in this case both OTFS and BPSK have the same CRB expression since the Doppler estimation does not depend on the signal waveform but on the received energy. The expression is thus given by,

$$\text{CRB}(\nu) = 3 \cdot \left(4\pi^2 \frac{E_s}{N_0/2}\right)^{-1} \tag{8}$$

The results for the Doppler estimation are shown in Fig. 4, where OTFS is shown to perform similarly to BPSK. By the same token as in the delay RMSE, the results are expected since OTFS should not provide a substantial gain with respect to spread-spectrum single-carrier BPSK in a scenario without multipath.

B. Performance for the LEO multipath channel

In this subsection we consider the two multipath scenarios described in Table I with the OTFS configuration in Table II. The received OTFS signal in the DD domain for the ν' in the first scenario, and considering an example $\tau' = 45$ m, is compared to the BPSK AF for this same signal in Fig. 5. The advantage of using OTFS in *doubly-spread* channels is clearly seen, since OTFS manages to discern the LOS and the multipath in both delay and Doppler domains, while BPSK cannot distinguish the multipath from the LOS since no Doppler differentiation can be achieved, and the LOS and multipath lobes end up coalescing, which distorts the main lobe of the LOS, and thus affects the estimation accuracy of both delay and Doppler. Even if in this case the OTFS LOS ends up without distortion because of the doubly-spread channel, it is noticeable that it only needs the various paths to be distinguishable in one of the two dimensions, and thus OTFS suffers from little error even if there is negligible delay difference, if the paths are separated in the Doppler dimension.

To analyse the multipath effect on positioning accuracy, it is common to obtain the Multipath Error Envelope (MEE), which provides the error that might be expected for a certain relative multipath delay with respect to the LOS. The MEE is a concept used in satellite navigation systems to describe the bounds of errors caused by multipath interference. Multipath interference occurs when a signal from a satellite reaches the receiver via multiple paths due to reflections off surfaces like buildings or the ground. This can cause errors in the position calculation.

The MEE provides an estimate of the maximum potential error introduced by these multipath effects. It is particularly important in urban environments where reflections are more common. The typical way to model MEE is to consider a LOS and a single multipath reflection, with variable spacing to the first path and typically at half of the amplitude of the first path and to investigate the effect of such varying multipath spacing on the positioning accuracy. We present the MEE results in meters, showing both the multipath delay (or replica delay) and the MEE as time (or delay) multiplied with the speed of light, for a more illustrative representation.

Fig. 6 shows the MEE for BPSK and OTFS for the LEO scenarios in Table I, and for the case of $\nu' = 0$ Hz. Notably, any ν' produces the same MEE for BPSK, due to the low resolution in the Doppler direction of the AF, while OTFS is capable of distinguishing the various paths through their differentiation in Doppler shift, which produces a very low MEE for OTFS in the considered LEO scenarios, and in general for any ν' larger than $\Delta\nu$.

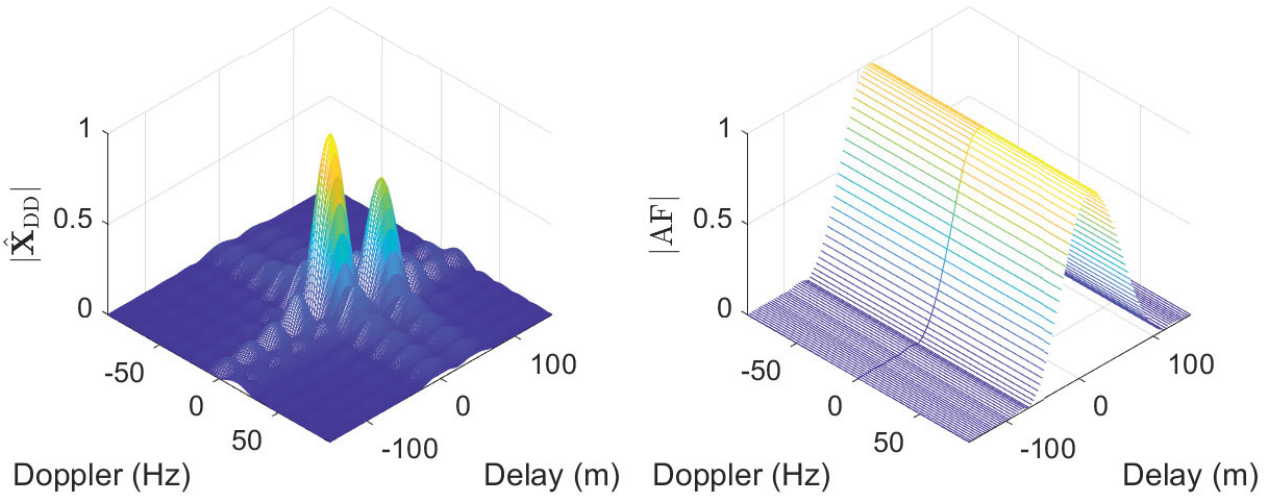

Fig. 5. OTFS signal at the DD domain at reception (left) and the ambiguity function of BPSK at reception (right) for a channel with *doubly-spread* multipath.

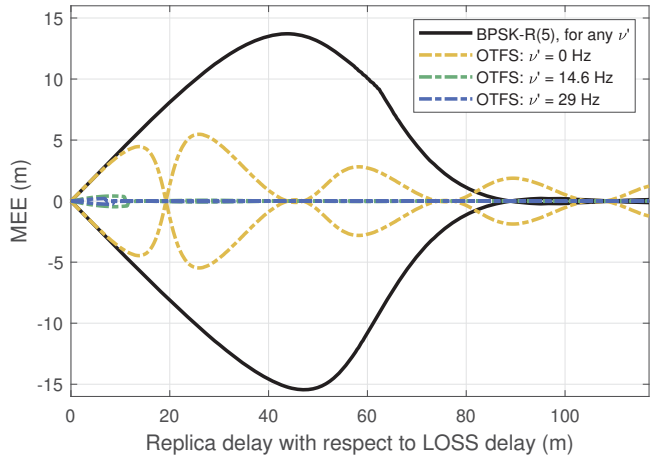

Fig. 6. Comparison of the Multipath Error Envelope between BPSK and OTFS.

VII. Conclusions

In conclusion, this paper has shown the prospect of using OTFS as a waveform solution for future LEO-PNT applications and air-to-ground propagation channels exhibiting large Doppler spreads. We have shown some of the capabilities of OTFS in terms of delay and Doppler estimation accuracy in comparison with a spread-spectrum single-carrier BPSK modulation, currently used in GNSS systems as well as with the theoretical CRB bound for an AWGN channel. We also studied the performance in multipath, focusing on multipath error envelopes for various LEO scenarios. Specifically, we have made use of the relative Doppler shift given by the fast-changing geometry of the LEO scenario, which makes the LEO channel *doubly-spread*. Under such assumption of doubly-spread channels, the OTFS waveform manages to distinguish the Doppler differences between the channel paths due to its improved Doppler resolution with respect to OFDM or any other modulation, which comes from its distinctive signal design. For this reason, the MEE of OTFS becomes increasingly small with bigger Doppler differences between paths and, with the proper setup of the OTFS configuration parameters (namely the bandwidth B, the number of subcarriers M, and the number of embedded OFDM symbols N), it becomes considerably small for LEO multipath channels and thus well suited for PNT applications. Our findings so far point out towards the fact that high positioning accuracy in multipath scenarios can be achieved with a proper configuration of OTFS, making it a potentially promising solution for LEO-PNT. Future research on LEO-PNT waveform design should also take into account how to optimize the signal acquisition and tracking in the presence of significant Doppler shifts and spreads, due to the high relative velocities between LEO satellites and ground receivers. LEO satellites often operate within constrained bandwidths, making thus essential to also optimise the waveforms to low bandwidths and to expand our work to bandwidths below 10 MHz. Last but not least, designing waveforms that can scale up with large constellations and integrate seamlessly with existing GNSS and communication systems [30] remains a significant challenge.

Acknowledgments

This work was supported by the Tampere University Dean's doctoral grant program and by the Jane and Aatos Erko Foundation and by Teknologiateollisuus 100-year Foundation, under the project INCUBATE. This work has also been supported by the LEDSOL project, funded within the LEAP-RE programme by the European Union's Horizon 2020 Research and Innovation Program under Grant Agreement 963530 and by the Academy of Finland grant agreement 352364, and partly supported by the Spanish Agency of Research (projects PDC2023-145858-I00 and PID2023-152820OB-I00).

REFERENCES

[1] K. Borre, I. Fernández-Hernández, J. A. López-Salcedo, and M. Z. H. Bhuiyan, *GNSS software receivers*. Cambridge University Press, 2022.

[2] E. D. Kaplan and C. J. Hegarty, *Understanding GPS, Principles and Applications. 3rd Edition*. Artech House, 2017.

[3] H. Benzerrouk, Q. Nguyen, F. Xiaoxing, A. Amrhar, A. V. Nebylov, and R. Landry, "Alternative PNT based on Iridium Next LEO Satellites Doppler/INS Integrated Navigation System," in *Int. Conf. on Integrated Navigation Syst.*, 2019, pp. 1–10.

[4] R. Morales Ferre, J. Praks, G. Seco-Granados, and E. S. Lohan, "A Feasibility Study for Signal-in-Space Design for LEO-PNT Solutions With Miniaturized Satellites," *IEEE Journal on Miniaturization for Air and Space Syst.*, vol. 3, no. 4, pp. 171–183, 2022.

[5] S. De Bast, J. Sleewaegen, and W. De Wilde, "Analysis of Multipath Code-Range Errors in Future LEO-PNT Systems," *Eng. Proc.*, vol. 54, no. 1, p. 34, 2023.

[6] J. Khalife, M. Neinavaie, and Z. M. Kassas, "The First Carrier Phase Tracking and Positioning Results With Starlink LEO Satellite Signals," *IEEE Trans. on Aerosp. and Electron. Syst.*, vol. 58, no. 2, 2022.

[7] J. J. Khalife and Z. M. Kassas, "Receiver Design for Doppler Positioning with Leo Satellites," in *ICASSP 2019 - 2019 IEEE International Conference on Acoustics, Speech and Signal Process. (ICASSP)*, 2019, pp. 5506–5510.

[8] F. Farhangian and R. Landry, "Multi-Constellation Software-Defined Receiver for Doppler Positioning with LEO Satellites," *Sensors*, vol. 20, no. 20, 2020.

[9] B. Eissfeller, T. Pany, D. Dötterböck, and R. Förstner, "A comparative study of leo-pnt systems and concepts," in *Proceedings of the ION 2024 Pacific PNT Meeting*, ser. PNT 2024. Institute of Navigation, May 2024. [Online]. Available: http://dx.doi.org/10.33012/2024.19646

[10] R. Hadani, S. Rakib, M. Tsatsanis, A. Monk, A. J. Goldsmith, A. F. Molisch, and R. Calderbank, "Orthogonal time frequency space modulation," in *IEEE Wireless Commun. and Net. Conf.*, 2017, pp. 1–6.

[11] Y. Liu, M. Chen, C. Pan, T. Gong, J. Yuan, and J. Wang, "OTFS vs OFDM: Which is Superior in Multiuser LEO Satellite Communications," https://arxiv.org/abs/2403.02012, 2024, [Accessed 09-09-2024].

[12] F. S. Prol, R. M. Ferre, Z. Saleem, P. Välisuo, C. Pinell, E. S. Lohan, M. Elsanhoury, M. Elmusrati, S. Islam, K. Çelikbilek, K. Selvan, J. Yliaho, K. Rutledge, A. Ojala, L. Ferranti, J. Praks, M. Z. H. Bhuiyan, S. Kaasalainen, and H. Kuusniemi, "Position, Navigation, and Timing (PNT) Through Low Earth Orbit (LEO) Satellites: A Survey on Current Status, Challenges, and Opportunities," *IEEE Access*, vol. 10, pp. 83 971–84 002, 2022.

[13] Z. Kassas, J. Morales, and J. Khalife, "New-age satellite-based navigation–STAN: simultaneous tracking and navigation with LEO satellite signals," *Inside GNSS Magazine*, vol. 14, no. 4, pp. 56–65, 2019.

[14] K. Celikbilek, E. S. Lohan, and J. Praks, "Optimization of a LEO-PNT constellation: Design considerations and open challenges," *Submitted to Wiley International Journal of Satellite Communications and Networking*, 8 2024. [Online]. Available: http://dx.doi.org/10.22541/au.172446847.77321818/v1

[15] D. Egea-Roca, J. A. López-Salcedo, G. Seco-Granados, and E. Falletti, "Comparison of Several Signal Designs Based on Chirp Spread Spectrum (CSS) Modulation for a LEO PNT System," *Proc. of the 34th International Technical Meeting of the Satellite Division of The Institute of Navigation (ION GNSS+ 2021)*, pp. 2804–2818, September 2021.

[16] P. A. Iannucci and T. E. Humphreys, "Economical fused leo gnss," in *2020 IEEE/ION Position, Location and Navigation Symposium (PLANS)*, 2020, pp. 426–443.

[17] F. Kunzi, B. Braun, M. Markgraf, O. Montebruck, and W. Frese, "First Steps Toward a Fully Operational LEO PNT Payload," InsideGNSS magazine, https://insidegnss.com/first-steps-toward-a-fully-operational-leo-pnt-payload/, 2024, [Accessed 09-09-2024].

[18] M. F. Keskin, H. Wymeersch, and V. Koivunen, "Mimo-ofdm joint radar-communications: Is ici friend or foe?" *IEEE Journal of Selected Topics in Signal Processing*, vol. 15, no. 6, pp. 1393–1408, 2021.

[19] P. H. Moose, "A technique for orthogonal frequency division multiplexing frequency offset correction," *IEEE Trans. on Commun.*, vol. 42, no. 10, pp. 2908–2914, 1994.

[20] M. F. Keskin, H. Wymeersch, and A. Alvarado, "Radar sensing with OTFS: Embracing ISI and ICI to surpass the ambiguity barrier," in *2021 IEEE International Conference on Commun. Workshops (ICC Workshops)*. IEEE, 2021, pp. 1–6.

[21] Q. Zheng, F. Wang, X. Chen, Y. Liu, D. Miao, and Z. Zhao, "Comparison of 5G waveform candidates in high speed scenario," in *22nd General Assem. and Scientific Symp. of the Int. Union of Radio Science*, 2017.

[22] S. K. Mohammed, R. Hadani, A. Chockalingam, and R. Calderbank, "OTFS—A Mathematical Foundation for Communication and Radar Sensing in the Delay-Doppler Domain," *IEEE BITS*, vol. 2, no. 2, 2022.

[23] L. Xiao, S. Li, Y. Qian, D. Chen, and T. Jiang, "An overview of OTFS for Internet of Things: Concepts, benefits, and challenges," *IEEE Internet of Things Journal*, vol. 9, no. 10, pp. 7596–7618, 2021.

[24] Hong, Yi and Thaj, Tharaj and Viterbo, Emanuele, *Delay-Doppler Communications: Principles and Applications*. Academic Press, 2022.

[25] J. Shi, Z. Li, J. Hu, Z. Tie, S. Li, W. Liang, and Z. Ding, "OTFS enabled LEO satellite communications: A promising solution to severe doppler effects," *IEEE Network*, 2023.

[26] P. Raviteja, E. Viterbo, and Y. Hong, "OTFS performance on static multipath channels," *IEEE Wireless Commun. Letters*, vol. 8, no. 3, 2019.

[27] A. Sharma, S. Jain, R. Mitra, and V. Bhatia, "Performance Analysis of OTFS Over Multipath Channels for Visible Light Communication," in *Int. Conf. on Commun., Signal Process. and their Applications*, 2021.

[28] *ETSI TS 138 101-1 5G NR User Equipment (UE) radio transmission and reception; Part 1: Range 1 Standalone*, ETSI, V17.12.0, 2024.

[29] R. Martin, "Comments on "OFDM Transmission for Time-Based Range Estimation"," *IEEE Signal Process. Letters*, vol. 18, no. 2, p. 144, 2010.

[30] I. Leyva-Mayorga, B. Soret, M. Röper, D. Wübben, B. Matthiesen, A. Dekorsy, and P. Popovski, "Leo small-satellite constellations for 5g and beyond-5g communications," *IEEE Access*, vol. 8, pp. 184 955–184 964, 2020.